Bulletin of the Seismological Society of America, Vol. 93, No. 3, pp. 1226–1234, June 2003

Near-Field Survey of the 1946 Aleutian Tsunami on Unimak and Sanak Islands

by Emile A. Okal, George Plafker, Costas E. Synolakis, and José C. Borrero

Abstract The 1946 Aleutian earthquake stands out among tsunamigenic events because it generated both very high run-up near the earthquake source region and a destructive trans-Pacific tsunami. We obtained new data on the distribution of its tsunami in the near field along south-facing coasts between Unimak Pass on the west and Sanak Island on the east by measuring the height of driftwood and beach materials that were deposited by the tsunami above the extreme storm tide level. Our data indicate that (1) the highest measured run-up, which is at the Scotch Cap lighthouse, was 42 m above tide level or about 37 m above present storm tide elevation; (2) run-up along the rugged coast from Scotch Cap for 12 km northwest to Sennett Point is 12–18 m, and for 30 km east of Scotch Cap to Cape Lutke it is 24–42 m; (3) run-up along the broad lowlands bordering Unimak Bight is 10–20 m, and inundation is locally more than 2 km; (5) run-up diminishes to 8 m or less at the southeast corner of Unimak Island; (6) no evidence was found for run-up above present storm tides (about 4–5 m above MLLW) on the Ikatan Peninsula or areas along the coast to the west; and (7) run-up above storm tide level in the Sanak Island group is restricted to southwest-facing coasts of Sanak, Long, and Clifford Islands, where it is continuous and locally up to 24 m high. Generation of the tsunami by one or more major earthquake-triggered submarine landslides near the shelf edge south of Unimak Island seems to be the only viable mechanism to account for the data on wave arrival time, run-up heights, and distribution, as well as for unconfirmed anecdotal reports of local postquake increases in water depth and diminished bottom-fisheries productivity. A preliminary hydrodynamic simulation of the local tsunami propagation and run-up using a dipolar model of a possible landslide off Davidson Bank provides an acceptable fit to the characteristics of the distribution of local run-up, with a value at 34 m at the Scotch Cap lighthouse.

Introduction

We present in this article a new dataset of near-field run-up and inundation measurements of the 1946 Aleutian tsunami, obtained during a 4-day field project on the islands of Unimak and Sanak in August 2001.

The exact origin of the great tsunami of 1 April 1946 in the Aleutian Islands remains controversial. The parent earthquake, whose epicenter relocates along the wall of the continental slope, at 53.33° N, 163.00° W (Fig. 1), features a conventional magnitude of only 7.4, as reported by Gutenberg and Richter (1954). Yet, its tsunami was catastrophic both in the near field, where it eradicated the Scotch Cap lighthouse on Unimak Island (Fig. 2), and in the far field, where it killed 159 people in Hawaii, inflicted severe damage in the Marquesas Islands, and reportedly caused destruction as far away as Antarctica (Fuchs, 1982). Kanamori (1972) pointed out the slow character of the parent earthquake rupture, a property later confirmed by Pelayo (1990), Okal (1992), Johnson and Satake (1997), and Okal *et al.* (2003). Due to the scarcity and poor quality of adequate seismic records, the static value of the moment of the earthquake remains somewhat unconstrained between 2×10^{28} and 8×10^{28} dyne cm. On the other hand, Kanamori (1985) has speculated that the 1946 event might have involved an underwater landslide, perhaps comparable to those documented during the 1929 Grand Banks, Newfoundland, 1953 Fiji, 1954 Orléansville, Algeria, and 1956 Amorgos, Greece, events (Heezen and Ewing, 1952, 1955; Ambraseys, 1960; Houtz, 1962), or inferred from a variety of evidence for the more recent 1998 Papua New Guinea (PNG) disaster (Synolakis *et al.,* 2002).

The eventual resolution of the exact nature of the mechanism of generation of the 1946 Aleutian tsunami, and in particular of the role played by any potential underwater landslide, will have important implications in terms of the

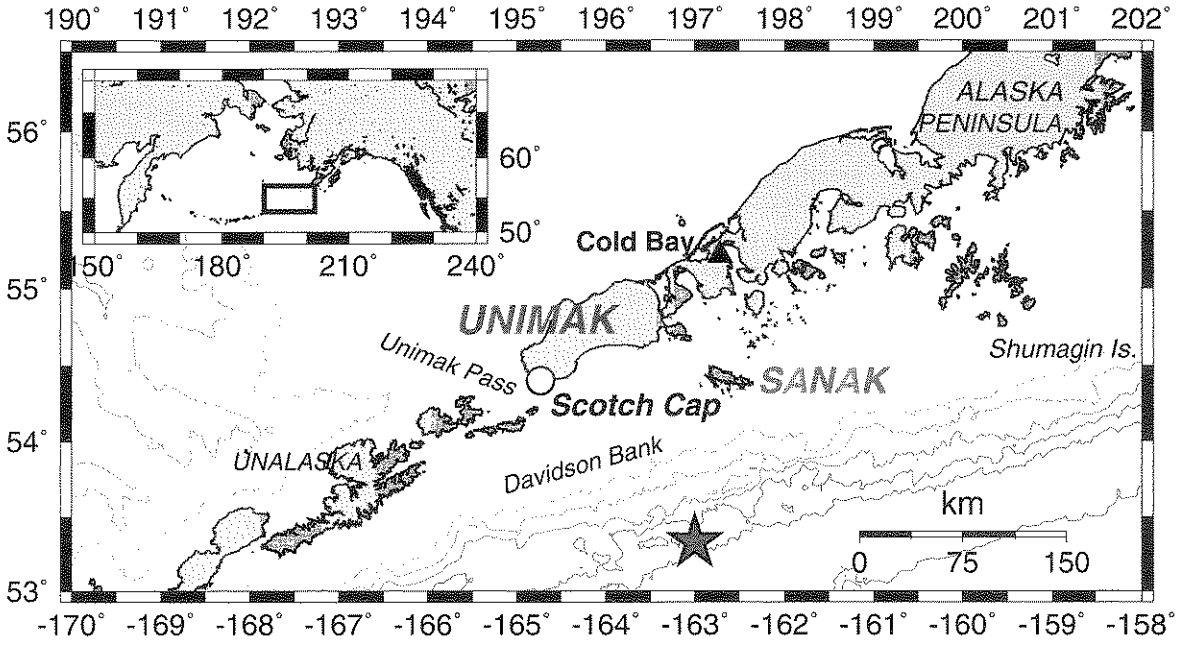

Figure 1. General map of the epicentral area of the 1946 Aleutian earthquake. The relocated epicenter (Okal and López, 2002) is shown as the large star. Also identified are the islands of Unimak and Sanak, visited during the survey, the location of the destroyed lighthouse at Scotch Cap (circle), and our base camp at Cold Bay (triangle). The inset locates the area of the main map (box) in the North Pacific. The interval of the bathymetric contours is 1000 m.

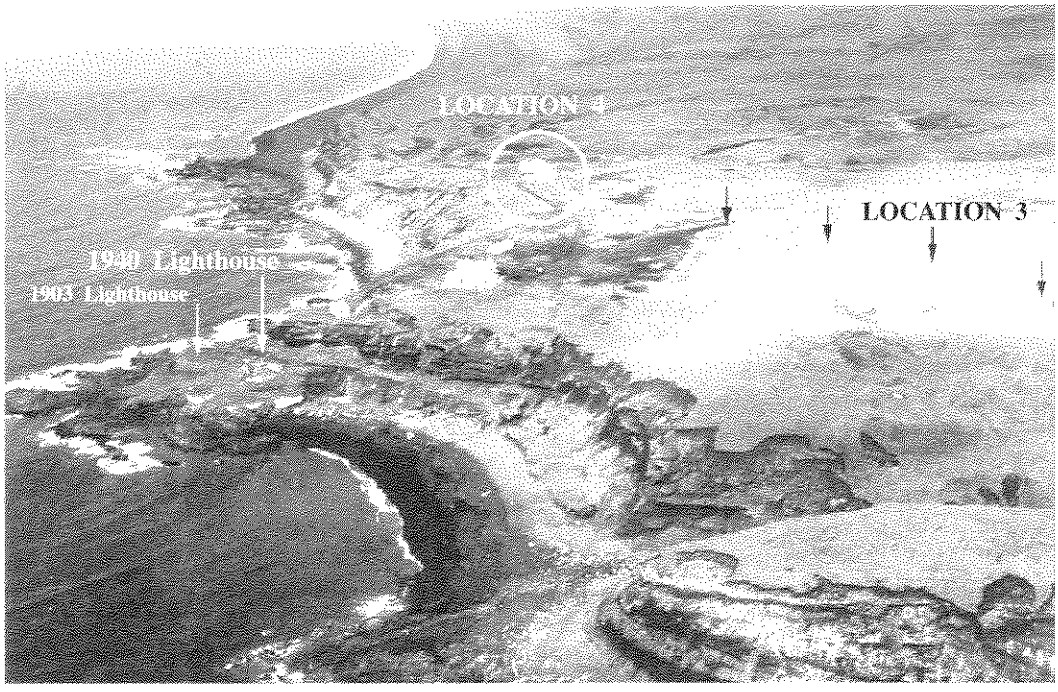

Figure 2. Oblique air view looking northwest at Scotch Cap station, taken in 1966 (photo: U.S. Coast Guard). The white arrows indicate the ruins of the concrete lighthouse destroyed by the tsunami (right arrow) and of a wooden predecessor (built in 1903, decommissioned in 1940; left arrow). The circled white building was the radio communication facility, flooded by the tsunami (Sanford, 1946), whose ruins constitute location 4. The three buildings in the foreground on the bluff postdate the tsunami. The dashed line and the black arrows show the inundation line identified by debris deposited by the tsunami. Maximum run-up is found at location 3.

evaluation of tsunami risk, in this and other geographic provinces. In very general terms, the amplitude of the far-field tsunami is largely controlled by the deformation of the ocean floor resulting from the seismic dislocation, while any underwater landslide would affect only the very near field (Okal and Synolakis, 2003). This point was particularly strongly illustrated in the case of the 1998 PNG event, whose tsunami was catastrophic in the near field but barely detectable in the far field (Synolakis *et al.,* 2002). In this respect, most previous investigations of the source of the 1946 tsunami modeled either the amplitudes (Pelayo, 1990) or the waveforms (Johnson and Satake, 1997) of tidal gage data available only in the far field, which explains that those studies concluded to the adequacy of a purely dislocative source. By contrast, the successful modeling of any possible landslide component to the source of the 1946 tsunami must use an adequate database of run-up values in the near field, since the far field remains essentially insensitive to this type of source. The present study describes such a database, obtained from fieldwork conducted over a 4-day window in August 2001, from a field base at Cold Bay, Alaska (Fig. 1) and with all local travel by helicopter. It follows in the footsteps of our previous fieldwork on the 1946 tsunami in the far field, in which we gathered a dataset of 54 run-up and inundation points through the interview of 48 elderly survivors on eight islands deprived of coral reefs of the central and South Pacific (Okal *et al.,* 2002c).

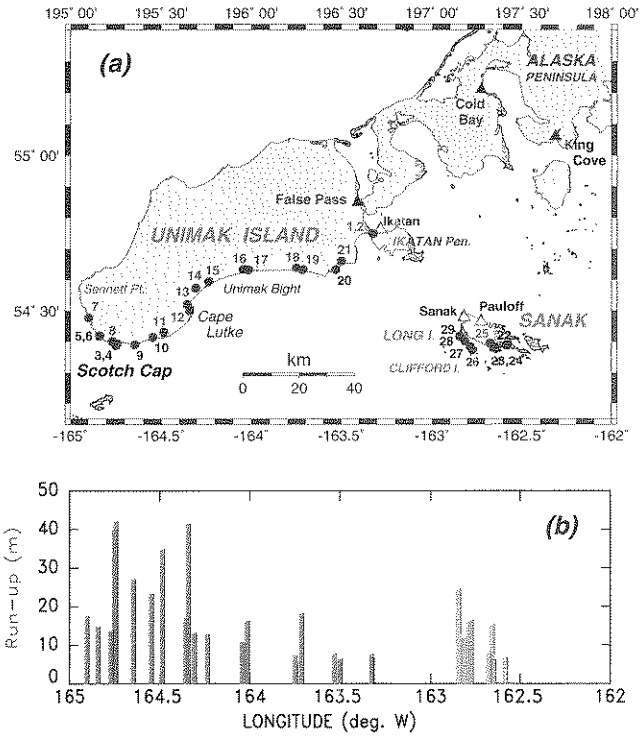

Figure 3. (a) Map of the field area, comprosed of the islands of Unimak and Sanak. The solid triangles are presently inhabited settlements; the open ones show the villages abandoned in the 1970s. Solid circles (with location numbers; see Table 1) represent the location of the watermarks measured in the present study. (b) Run-up values (corrected for tides) along the coasts of Unimak and Sanak plotted as a function of longitude at the watermark.

Methodology

The eastern Aleutian Islands are very sparsely populated, with only one permanent settlement on Unimak Island, the village of False Pass on the narrow straits separating the island from the southwestern tip of the Alaska Peninsula (Fig. 3a). On Sanak Island, two villages (Sanak and Pauloff, located on the west and north coasts, respectively) were populated in 1946, but abandoned in the 1970s. As a result, the nature of our watermarks, as well as our general *modus operandi,* had to be significantly adapted from our previous surveys in the far field, which were based exclusively on the interviews of elderly witnesses. In the present study, we base our observations on several pieces of evidence and circumstances. At Scotch Cap lighthouse, we can rely on the detailed Coast Guard report by the chief radio electrician at the radio station on the terrace overlooking the lighthouse (Sanford, 1946) and on the interpretation of aerial photographs (e.g., Fig. 2). While the latter was totally destroyed, the former was merely flooded to the extent that power was lost from shorted generators. Historical photographs document the destruction of the building housing the radio station in the 1970s, but its ruins are easily identified on the bluff and therefore constitute a watermark.

An additional and extremely important fact is that no trees grow on the eastern Aleutian Islands, on the Alaska Peninsula west of the Kodiak-Shelikof Straits (158° W), or on any of the offshore islands, the tallest local vegetation consisting of shrubs. Therefore, any large logs, tree trunks, or stumps found on the islands (Fig. 4), tens of kilometers away from any human settlement, must be considered erratic, the only possible depositional agent being the sea. The farthest penetration of storm surges is generally identifiable as a discontinuous line of debris that defines the extreme storm tide elevation, usually within a few tens of meters of the shoreline. Thus, their action can be discarded at elevations of several meters above this line and at distances of hundreds of meters inland, where pieces of driftwood can be identified unambiguously as tsunami deposits. We base their association with the 1946 event on two lines of evidence: On Unimak Island, we were able to follow samples of similarly preserved driftwood for a distance of 80 km along the southern coast of the island, thus establishing continuity with the watermark at Scotch Cap lighthouse, for which a definitive association with the 1946 tsunami is available from the Coast Guard report (Sanford, 1946). On Sanak Island, we relied on the testimony of an elderly witness (aged 10 in 1946, then a resident of Sanak Village, now living in False Pass), who confirmed to us during a videotaped interview that major pieces of driftwood had been deposited above storm tide level on southern Sanak Island and Long

Figure 4. Examples of driftwood watermarks surveyed in the present study. Top: Location 12, north of Cape Lutke, Unimak Island, view to the east; 13 August 2001. Bottom: Location 29, Long Island (Sanak), view to the southeast; 15 August 2001.

Island by the 1946 tsunami. We also know from these same sources, as well as from tidal gage data, that the 1946 tsunami had significantly higher amplitudes, especially in the Aleutian Islands, than generated by any of the large subsequent earthquakes (Aleutian 1957, $M_0 \geq 8.5 \times 10^{28}$ dyne cm; Alaska 1964, $M_0 = 8.2 \times 10^{29}$ dyne cm; Aleutian 1965, $M_0 = 1.2 \times 10^{29}$ dyne cm, as summarized in Okal [1992]).

Once a watermark was identified we determined *inundation*, that is, distance to the nearest point on the shoreline, and *run-up*, that is, the vertical penetration of the wave at the watermark. Given the large inundation distances over which measurements had to be taken (more than 2 km along Unimak Bight), the potentially hazardous conditions (Unimak Island has a large colony of grizzly bears and Sanak Island herds of feral bovines) and the short time available, surveys using on-land level transects, used traditionally in previous tsunami surveys, were not feasible. Rather, inundation was computed from differences in Global Positioning System fixes between the watermark and the nearest shore, and run-up was obtained from differences in elevation measurements taken at the watermark and the shoreline, using the average of two readings on digital barometric altimeters, deployed side by side at each location for redundancy, with the two sites occupied within a few minutes of each other, thus minimizing the effect of weather-induced fluctuations in atmospheric pressure. Because tsunami deposits had to be above the extreme high storm tide line to be visible, our lower limit of detection was $\sim 5 \pm 1$ m above tide level at the tsunami arrival time. We estimate the precision of our measurements at ± 1 m vertically and 3% (from 2 to 60 m) horizontally. Finally, note that the run-up values measured at the watermarks are actually minima, since they relate to ground surface on which driftwood was deposited. In the case of large logs or root boles (such as in Fig. 4), the water depth at the site had to be sufficient to move these objects.

The raw run-up data were referred to the sea level prevailing at the time of the measurement, and a tide correction (ranging from -0.4 to $+1.1$ m) later implemented in order to correctly estimate the amplitude of the tsunami over the tide at the time of inundation.

Results

The resulting dataset is listed in Table 1 and plotted as a function of longitude on Figure 3b. Our maximum run-up value is 42 m at Scotch Cap, near the ruins of the radio station (Fig. 2). This value is significantly greater than those routinely reported in the literature (30–35 m). Farther east, run-up amplitudes of 30–40 m are found consistently on the southwestern coast of Unimak, between Scotch Cap and Cape Lutke, while values fall below 20 m along Unimak Bight.

At Sanak Island, we measured run-up values of 15–24 m on Long Island (Fig. 3b) and 7–15 m on the southeastern side of Sanak proper. Again, these amplitudes are significantly larger than the 5–6 m previously reported (Fryer and Watts, 2000), which relate to the two villages in sheltered bays on the northern coast.

We found no evidence of watermarks above the storm tide line east of False Pass, on Ikatan Peninsula, or on the southern Alaska Peninsula and its offshore islands. Furthermore, eyewitness accounts indicate no inundation above storm tide lines at the villages of Cold Bay and King Cove.

Inundation

Inundation values at the 29 sites surveyed are reported in Table 1. They range from 62 m on Sanak to 2217 m at location 16 along Unimak Bight. The value given for locations 1 and 2 (510 m) represents the width of the narrow beach bar connecting Ikatan Peninsula to the mainland of Unimak Island. Reports from an eyewitness interviewed at False Pass indicated that the lowest part of the isthmus was washed over by the tsunami in the vicinity of the abandoned Ikatan village. The inundation data are strongly scattered, in direct relationship to the morphology of the seashore, varying from a flat beach backed by gently rising slopes along

Table 1
Run-Up and Inundation Dataset Obtained in This Study

Location Number	Latitude (°N)	Longitude (°E)	Run-Up above 2001 Waterline (m)	Tidal Correction (m)	Corrected Run-Up (m)	Inundation (m)	Geographic Location
Unimak Island							
1	54.75023	−163.31963	7.5	−0.8	6.7	510	Ikatan Village site
2	54.75033	−163.32344	7.6	0.0	7.6	510	Ikatan Village Site
3	54.39437	−164.74113	42.2	0.0	42.2	190	Scotch Cap, east of radio station site
4	54.38835	−164.74759	39.8	0.0	39.8	180	Scotch Cap, radio station
5	54.42010	−164.83913	15.3	−0.4	14.9	127	Northwest of Scotch Cap
6	54.41947	−164.83975	12.5	−0.3	12.1	100	Northwest of Scotch Cap
7	54.47850	−164.90059	17.9	−0.3	17.6	171	South of Sennett Point
8	54.40158	−164.76839	14.0	−0.2	13.8	190	Northwest of Scotch Cap
9	54.39090	−164.64601	27.4	−0.2	27.2	330	Seal Cape
10	54.41620	−164.54697	23.6	−0.1	23.5	570	Northeast of Arch Point
11	54.43227	−164.48651	34.9	−0.1	34.8	890	East of Promontory Hill
12	54.50110	−164.34103	40.5	1.1	41.6	412	North of Cape Lutke
13	54.52151	−164.35620	16.2	0.9	17.1	1230	Promontory Cove
14	54.57373	−164.30673	12.4	0.8	13.2	1965	Western Unimak Bight
15	54.59425	−164.23357	12.2	0.6	12.8	728	Western Unimak Bight
16	54.63403	−164.04332	10.4	0.4	10.8	2217	Northwest of Cape Rukavitsie
17	54.63283	−164.01404	16.1	0.3	16.4	1837	Northeast of Cape Rukavitsie
18	54.63903	−163.75105	7.3	0.1	7.4	634	Brown Peak
19	54.63323	−163.71565	18.3	−0.1	18.2	330	East of Brown Peak
20	54.63388	−163.53073	8.0	−0.2	7.8	285	South of Lazaref Peak
21	54.66105	−163.49944	6.8	−0.4	6.4	1077	North of Lazaref Peak
Sanak and Long Islands							
22	54.38908	−162.57817	6.4	0.3	6.7	131	East of Salmon Bay, Sanak
23	54.37707	−162.64110	5.9	0.3	6.2	90	Southeast of Sandy Bay, Sanak
24	54.38003	−162.64938	15.0	0.3	15.3	62	Southeast of Sandy Bay, Sanak
25	54.39605	−162.66943	7.5	0.3	7.8	291	Sandy Bay, Sanak
26	54.37447	−162.76926	16.3	0.3	16.6	197	Clifford Island southeast (Long Island)
27	54.38335	−162.78212	15.8	0.3	16.1	228	Clifford Island southwest (Long Island)
28	54.40213	−162.81288	11.5	0.3	11.8	96	Long Island (center)
29	54.41785	−162.84265	24.3	0.3	24.6	97	Long Island (northwest)

Unimak Bight to cliffs and embankments at Scotch Cap, Cape Lutke, and to a lesser extent along the coast of Sanak.

Discussion

Distribution of Run-Up and Its Aspect Ratio

The database of run-up values presented in Table 1 and Figure 3b lends itself to comparison with similar datasets gathered in the aftermath of recent tsunamis. Of particular interest for the identification of the source of the tsunami is the lateral distribution of run-up along the near-field shore. We have shown in Okal *et al.* (2002a) that the aspect ratio A of this distribution can be used as a discriminant between tsunamis generated by seismic dislocations and by underwater landslides, the physical argument being that, for an earthquake, A is directly controlled by the strain released on the fault, which is itself limited by the mechanical properties of the rupturing material. On the other hand, for an underwater landslide, A is controlled by the ratio of the amplitude of the original depression at the sea surface to its horizontal extent, which can be several orders of magnitude larger than the maximum strain release in crustal rocks (Okal and Synolakis, 2003). Figure 5 plots the Unimak dataset projected along the azimuth N71 °E, which is representative of the general direction of the eastern Aleutian coastline (we exclude the Sanak data points from the plot). We compute the aspect ratio $A = b/a$ by fitting a curve of the form

$$\zeta = \frac{b}{\left(\frac{x - c}{a}\right)^2 + 1}, \qquad (1)$$

where ζ is the run-up amplitude at abscissa x along the shore. As summarized on Figure 5, the value for Unimak, $A = 6.4 \times 10^{-4}$, compares very favorably with the aspect ratio derived for the 1998 PNG event (4.8×10^{-4}) and is more than an order of magnitude greater than either simulated numerically for various geometries of dislocations (Hoffman *et al.*, 2002) or observed, for example, in the case of the 1992 Nicaragua and 2001 Peru tsunamis (Okal *et al.*, 2002b). This result must be considered tentative in view of the irregularity of the Unimak coastline (as compared to the much more linear geometries in PNG and Peru) and of the absence of

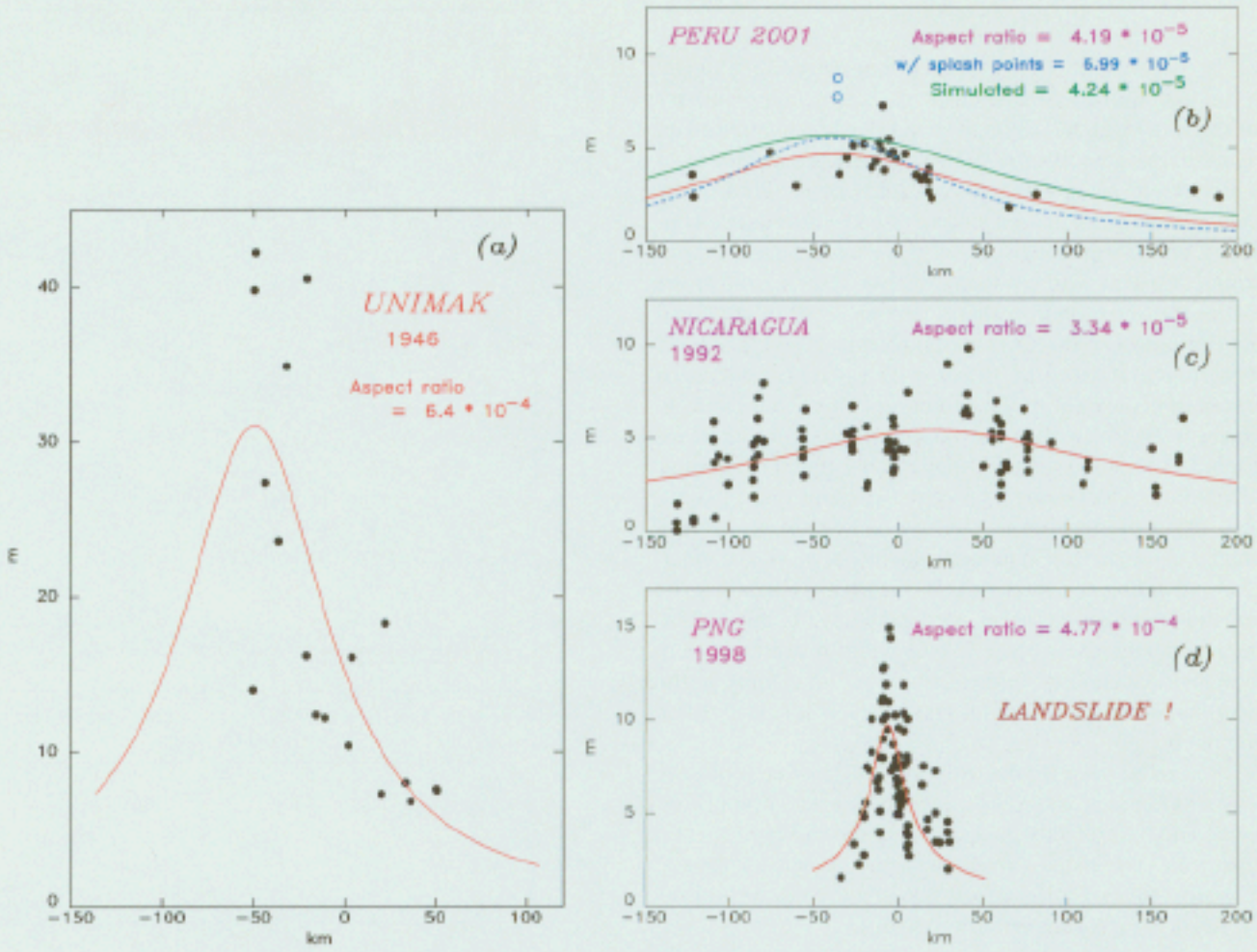

Figure 5. (a): Distribution of run-up values (solid dots) on Unimak Island plotted as a function of distance measured along the average azimuth (N71°E) of its southern shore. The red curve is the best-fitting equation (1) from which the aspect ratio A is computed. Right: Same as (a) for the 2001 Peru (b), 1992 Nicaragua (c), and 1998 PNG events (d) (adapted from Okal *et al.* (2002b)). In the case of the 2001 event, the red curve is obtained after suppressing two excessive values resulting from the wave having splashed against a cliff. The green curve is the result of a theoretical simulation (Hoffman *et al.*, 2002). Note that the Unimak dataset is most comparable to that for PNG (1998), where the tsunami was due to a submarine landslide (Synolakis *et al.*, 2002). By contrast, the 1992 and 2001 events have aspect ratios at least 1 order of magnitude smaller. The ratio of the horizontal and vertical scales is common to all plots, thus allowing direct comparison of the shapes of the curves.

data to the west of Scotch Cap; nevertheless, it supports the model of a landslide rather than an elastic dislocation as the source of the near-field tsunami.

This scenario, under which a landslide took place during or immediately after the 1946 earthquake, would be legitimate given that surveys using the GLORIA long-range side-scan sonar have documented significant slumps along most segments of the Aleutian margin, notably off Unalaska to the west of Unimak (Dobson *et al.*, 1996). Indeed, Fryer and Watts (2000) have interpreted GLORIA data as defining slumps in the vicinity of Davidson Bank. It is also supported by anecdotal evidence from elderly fishermen now retired in False Pass and King Cove, who recalled during interviews a substantial impact on halibut fishing operations off Davidson Bank in the aftermath of the tsunami, which they attributed to "deepening of the sea floor." One of the witnesses reported to us that their observations were corroborated at the time by U.S. Navy personnel, who reported that depths increased by as much as 600 m (2000 ft), from post-tsunami *en route* soundings offshore from Unimak Island.

We must stress that this proposed scenario remains speculative and that the definite confirmation of the presence, nature, and age of a slide will require a dedicated marine survey.

Preliminary Modeling

In this context, we use here a preliminary slide model to run a simplified simulation of the interaction of the resulting wave with the Unimak shoreline. As summarized on Figure 6, our computation follows closely the method used in Borrero *et al.* (2001) and Synolakis *et al.* (2002). The initial condition of the sea surface is taken as a dipole consisting of a 28-m trough and a 19-m hump, these figures being consistent with a possible 600-m vertical drop at the continental slope, with a slump moving at 30 m/sec (Tinti and Bortolucci, 2000; Okal and Synolakis, 2003). The lever of the dipole is taken as 35 km, which is representative of the horizontal extent of the continental slope to the trench, where it is likely that the slump abutted or otherwise stopped. The initial deformation features a sech^2 transverse distribution. The propagation of the tsunami is then simulated using the technique of Titov and Synolakis (1998), which solves the full nonlinear shallow-water wave equations, including the modeling of run-up by extending the simulation domain over wet overland points. In this preliminary computation, we use a grid with an average 5-min bathymetric sampling, further refined in the vicinity of the coastline to as little as 200 m. This model is schematized on Figure 6b.

Figure 6a presents the distribution of run-up along the coasts of Unimak and Sanak, plotted as a function of longitude and thus directly comparable to the surveyed data on Figure 3b. While the simulated values remain in general somewhat lower than observed (by about 25%), the following features reproduce our observations:

1. The maximum run-up is observed at Scotch Cap lighthouse and Cape Lutke.
2. The run-up at Scotch Cap lighthouse is modeled at 34 m, an acceptable approximation to the observed 42 m. By contrast, a preliminary model run for a seismic dislocation featuring a slip of 10 m, considered the greatest allowable for a seismic moment of at most 8×10^{28}, produced a maximum initial deformation of the ocean floor of 5.6 m and a maximum run-up of only 7 m along the coast of Unimak. This relatively low value of run-up expresses the destructive interference in the near field created by the large extent of the dislocation source; only in the far field can the interference become constructive in the direction perpendicular to fault length, where phase time to a distant receiver is essentially constant for all elements of the source (Ben-Menahem and Rosenman, 1972).
3. The general shape of the run-up distribution (sustained between Scotch Cap and Cape Lutke, lower along western Unimak Bight) is reproduced.
4. Run-up on western Sanak reaches 20–25 m.

In conclusion, and notwithstanding a simulated run-up larger than observed at the eastern end of Unimak Bight, we reproduce both the order of magnitude of the observed run-up amplitudes and their distribution along the coasts. As such, this simple simulation experiment based on a crude bathymetric grid does support the model of one or more large landslides as the source of the near-field tsunami.

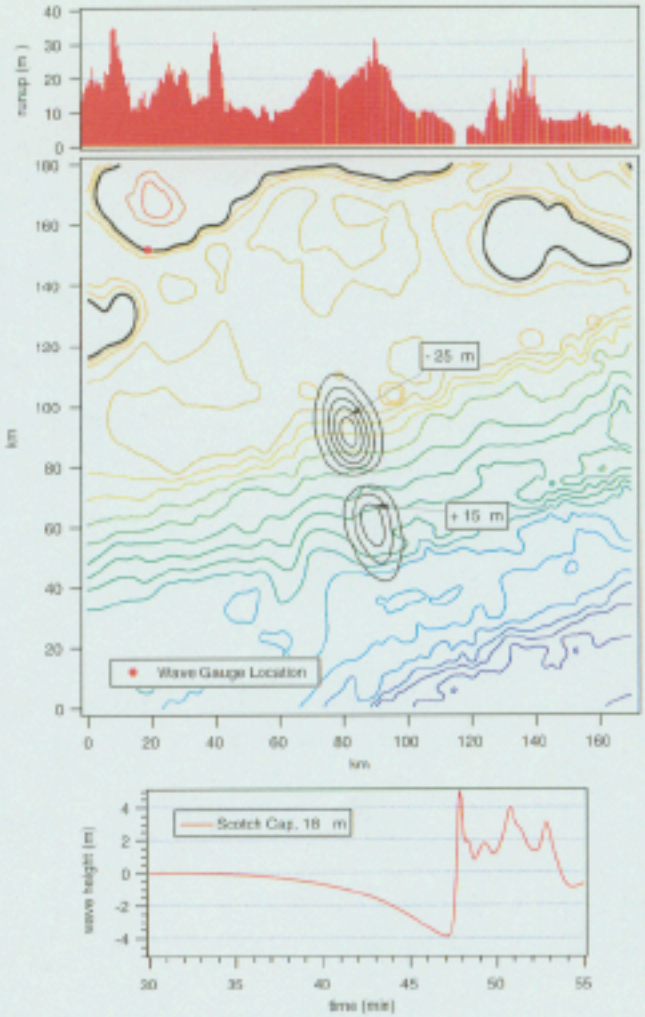

Figure 6. Center: Sketch of the initial model used in the preliminary modeling of the near-field tsunami. The colored contours are isobaths, at 100-m intervals down to 500 m and at 500-m intervals deeper. The positive and negative poles of the source dipole are contoured in black at 5-m intervals. The red dot indicates the location of the gauge simulated in the bottom frame. Top: Run-up computed along the coastline of Unimak and Sanak Islands, plotted as a function of distance in the east–west direction. Note the maxima obtained at Scotch Cap and Cape Lutke. Bottom: Synthetic wave amplitude at a simulated gauge located in front of Scotch Cap. Note the progressive drawdown, followed by a strong positive wave 48 min after initial time.

Finally, Figure 6c is a time series of the arrival of the wave at a simulated gauge located above the 18-m isobath in front of the Scotch Cap lighthouse. An important aspect of this plot is the timing of the first positive wave, which arrives 48 min after origin time. Sanford (1946) reported the

inundation of the radio station at 02:18 local time (13:18 GMT), 49 min after the relocated origin time of the mainshock (12:28:59 GMT [Okal and López, 2002]). This suggests that the generation of the wave, and hence the landslide, were coeval with the mainshock, if one keeps in mind the significant duration (at least 90 sec) of the latter's rupture. We have verified that this result is robust (within a few minutes) with respect to translation of the source along the steep continental slope off Davidson Bank, the only possible location for a major underwater landslide. The immediate triggering of the proposed landslide by the mainshock is in contrast to the case of the 1998 PNG tsunami, for which a 13-min gap existed between the two phenomena (Synolakis *et al.*, 2002). This variability in the triggering process simply expresses its highly nonlinear nature.

Figure 6 also suggests that the catastrophic inundation at Scotch Cap lighthouse was preceded by a large drawdown, although to our knowledge, no such phenomenon has been documented. In the midst of a moonless night (a new moon occurred on 2 April at 04:38 GMT), it may have been noticeable only to the staff of the lighthouse (a few minutes before they met their tragic fate), who had earlier noticed the coseismic uplift following the mainshock and reported it by telephone to the radio station before the arrival of the tsunami and consequent destruction of the lighthouse (Sanford, 1946).

Conclusion

Measurements taken on preserved watermarks of the 1946 tsunami on Unimak and Sanak Islands confirm the exceptional amplitude of run-up at Scotch Cap lighthouse (42 m) and document comparable values over a relatively short stretch of coastline extending northeastward 35 km to Cape Lutke. Substantial run-up heights reaching 25 m are also found on Long Island, on the southwestern shore of Sanak. Both the amplitude of the run-up and its spatial distribution are characteristic of the near field of a tsunami generated by a landslide rather than by a dislocation, a conclusion upheld by a preliminary numerical simulation and also supported by tentative evidence from elderly fishermen.

While this scenario will have to be authentificated by *in situ* marine geological and geophysical exploration, our results are in contrast to our previous work in the far field (Okal *et al.*, 2002c), where in particular the strong directivity of the tsunami required generation by a seismic dislocation. Thus, the emerging picture of the source of this most dramatic tsunami is that of a very slow seismic dislocation, sharing the general properties of such "tsunami earthquakes" as Nicaragua (1992) or Java (1994), albeit with a much larger moment probably reaching 8×10^{28} dyne cm (Okal and Lopez, 2002), which triggered coseismically a massive landslide at the edge of Davidson Bank. As previously modeled, the dislocation source can explain the generation of the far-field tsunami, while the landslide generated the exceptional amplitudes in the near field.

The presence of the landslide is not by itself singular: earthquakes routinely trigger landslides, both on land (e.g., Peru, 1970; Chi-Chi, Taiwan, 1999; El Salvador, 2001) and at sea, where they can locally enhance the run-up of tsunami waves to devastating amplitudes (e.g., 26 m at Riangkroko during the Flores Sea tsunami of 1992 (Imamura *et al.*, 1995)), but only over very limited distances (usually at most a few kilometers). The unique character of the run-up along the southern shore of Unimak probably reflects an exceptional volume for the landslide, which in the crude model of Figure 6 would total at least 200 km^3.

Acknowledgments

We thank the residents of Cold Bay, False Pass, and King Cove for their warm welcome and for willingly sharing with us their precious memories of the 1946 tsunami. Sam Egli skillfully flew us over the often fog-shrouded coastlines of the islands. The article was significantly improved through constructive reviews by Kenji Satake and Jean Johnson. This research was supported by the National Science Foundation. Some figures were generated using the GMT software (Wessel and Smith, 1991).

References

Ambraseys, N. N. (1960). The seismic sea wave of July 9, 1956 in the Greek archipelago, *J. Geophys. Res.* **65,** 1257–1265.

Ben-Menahem, A., and M. Rosenman (1972). Amplitude patterns of tsunami waves from submarine earthquakes, *J. Geophys. Res.* **77,** 3097–3128.

Borrero, J. C., J. F. Dolan, and C. E. Synolakis (2001). Tsunamis within the Eastern Santa Barbara Channel, *Geophys. Res. Lett.* **28,** 643–646.

Dobson, M. R., H. A. Karl, and T. L. Vallier (1996). Sedimentation along the fore-arc region of the Aleutian Island arc, Alaska, in *Geology of the United States' Seafloor,* J. V. Gardner, M. E. Field, and D. C. Twichell (Editors), Cambridge U Press, New York, 219–304.

Fryer, G. J., and P. Watts (2000). The 1946 Unimak tsunami: near-source modeling confirms a landslide (abstract), *EOS* **81** (48), F748–F749.

Fuchs, Sir V. (1982). Of ice and men: The story of the British Antarctic Survey, 1943–73, Anthony Nelson, Oswestry, 383 pp.

Gutenberg, B., and C. F. Richter (1954). *Seismicity of the Earth and Associated Phenomena,* Princeton University Press, Princeton, New Jersey, 310 pp.

Heezen, B. C., and W. M. Ewing (1952). Turbidity currents and submarine slumps, and the 1929 Grand Banks [Newfoundland] earthquake, *Amer. J. Sci.* **250,** 849–873.

Heezen, B. C., and W. M. Ewing (1955). Orléansville earthquake and turbidity currents, *Bull. Am. Assoc. Petrol. Geol.* **39,** 2505–2514.

Hoffman, I., C. E. Synolakis, and E. A. Okal (2002). Systematics of the distribution of tsunami run-up along coastlines in the near-field for dislocation sources with variable parameters (abstract), *EOS* **83** (22), WP54.

Houtz, R. E. (1962). The 1953 Suva earthquake and tsunami, *Bull. Seism. Soc. Am.* **52,** 1–12.

Imamura, F., E. Gica, T. Takahashi, and N. Shuto (1995). Numerical simulation of the 1992 Flores tsunami: interpretation of tsunami phenomena in Northeastern Flores Island and damage at Babi Islands, *Pure Appl. Geophys.* **144,** 555–568.

Johnson, J. M., and K. Satake (1997). Estimation of seismic moment and slip distribution of the April 1, 1946, Aleutian tsunami earthquake, *J. Geophys. Res.* **102,** 11,765–11,774.

Kanamori, H. (1972). Mechanisms of tsunami earthquakes, *Phys. Earth Planet. Interiors,* **6,** 346–359.

Kanamori, H. (1985). Non-double-couple seismic source (abstract), in *Proc. of the 23rd General Assembly of the International Assoc. Seismol. Phys. Earth Interiors,* Tokyo, 425.

Okal, E. A. (1992). Use of the mantle magnitude M_m for the reassessment of the seismic moment of historical earthquakes. I. Shallow events, *Pure Appl. Geophys.* **139,** 17–57.

Okal, E. A., and A. M. López (2002). New seismological results on the 1946 Aleutian earthquake (abstract), *EOS* **83** (22), WP54.

Okal, E. A., and C. E. Synolakis (2003). Theoretical comparison of tsunamis from dislocations and landslides, *Pure Appl. Geophys.* **160** (in press).

Okal, E. A., J. C. Borrero, and C. E. Synolakis (2002a). Solving the puzzle of the 1998 Papua New Guinea tsunami: the case for a slump, in *Solutions to Coastal Disasters,* L. Wallendorf and L. Ewing (Editors), American Society of Civil Engineering, 863–877.

Okal, E. A., L. Dengler, S. Araya, J. C. Borrero, B. Gomer, S. Koshimura, G. Laos, D. Olcese, M. Ortiz, M. Swensson, V. V. Titov, and F. Vegas (2002b). A field survey of the Camana, Peru tsunami of June 23, 2001, *Seism. Res. Lett.* **73,** 904–917.

Okal, E. A., C. E. Synolakis, G. J. Fryer, P. Heinrich, J. C. Borrero, C. Ruscher, D. Arcas, G. Guille, and D. Rousseau (2002c). A field survey of the 1946 Aleutian tsunami in the far field, *Seism. Res. Lett.* **73,** 490–503.

Okal, E. A., P.-J. Alasset, O. Hyvernaud, and F. Schindelé (2003). The deficient *T* waves of tsunami earthquakes, *Geophys. J. Int.* **152,** 416–432.

Pelayo, A. M. (1990). Earthquake source parameter inversion using body and surface waves: applications to tsunami earthquakes and to Scotia Sea seismotectonics, *Ph.D. Thesis,* Washington University, St. Louis.

Sanford, H. B. (1946). Log of Coast Guard Unit Number 368, Scotch Cap DF station, relating to the Scotch Cap light station tragedy of 1946, U.S. Coast Guard, Washington, D.C., 11 pp.

Synolakis, C. E., J.-P. Bardet, J. C. Borrero, H. L. Davies, E. A. Okal, E. A. Silver, S. Sweet, and D. R. Tappin (2002). The slump origin of the 1998 Papua New Guinea tsunami, *Proc. R. Soc. London A* **458,** 763–789.

Tinti, S., and E. Bortolucci (2000). Energy of water waves induced by submarine landslides, *Pure Appl. Geophys.* **157,** 281–318.

Titov, V. V., and C. E. Synolakis (1998). Numerical modeling of tidal wave runup, *J. Waterway Port Coast. Ocean Eng.* **124,** 157–171.

Wessel, P., and W. H. F. Smith (1991). Free software helps map and display data, *EOS* **72,** 441 and 445–446.

Department of Geological Sciences
Northwestern University
Evanston, Illinois 60201
(E.A.O.)

U.S. Geological Survey
345 Middlefield Road
Menlo Park, California 94025
(G.P.)

Department of Civil Engineering
University of Southern California
Los Angeles, California 90089
(C.E.S., J.C.B.)

Manuscript received 17 September 2002.